



Contents lists available at ScienceDirect

Bioorganic & Medicinal Chemistry Letters

journal homepage: www.elsevier.com/locate/bmcl

Discovery of 3,5-disubstituted-1*H*-pyrrolo[2,3-*b*]pyridines as potent inhibitors of the insulin-like growth factor-1 receptor (IGF-1R) tyrosine kinase

Samarjit Patnaik^{a,*}, Kirk L. Stevens^a, Roseanne Gerding^a, Felix Deanda^b, J. Brad Shotwell^a, Jun Tang^a, Toshihiro Hamajima^c, Hiroko Nakamura^c, M. Anthony Leesnitzer^a, Anne M. Hassell^a, Lisa M. Shewchuck^b, Rakesh Kumar^d, Huangshu Lei^a, Stanley D. Chamberlain^a

^a GlaxoSmithKline, Oncology R&D, 5 Moore Drive, Research Triangle Park, NC 27709, USA

^b GlaxoSmithKline, Computational and Structural Chemistry, 5 Moore Drive, Research Triangle Park, NC 27709, USA

^c GlaxoSmithKline, K. K. Tsukuba Research Laboratories, 43 Wadai Tsukuba, Ibaraki 300-4247, Japan

^d GlaxoSmithKline, Oncology R&D, 1250 S. Collegeville Road, Collegeville, PA 19426, USA

ARTICLE INFO

Article history:

Received 22 October 2008

Revised 22 December 2008

Accepted 30 December 2008

Available online 6 January 2009

Keywords:

IGF-1R

IGF-1R

Pyrrolopyridine

Kinase inhibitor

ABSTRACT

Exploration of the SAR around a series of 3,5-disubstituted-1*H*-pyrrolo[2,3-*b*]pyridines led to the discovery of novel pyrrolopyridine inhibitors of the IGF-1R tyrosine kinase. Several compounds demonstrated nanomolar potency in enzyme and cellular mechanistic assays.

© 2009 Published by Elsevier Ltd.

The overexpression or autoactivation of the insulin-like growth factor-1 receptor (IGF-1R) tyrosine kinase has been associated with various cancers.¹ High plasma levels of IGF-1 and low levels of IGF binding protein-3, which controls the amount of free circulating IGF, are directly correlated with an increased risk for developing colon, breast, prostate and lung cancer.² Several antagonists of the IGF-1 signaling pathway in the form of IGF-1R antibodies and small molecules are currently being investigated in clinical trials.³ Structurally diverse preclinical small molecule inhibitors of IGF-1R have also been reported and hold promise as useful antineoplastic agents.⁴

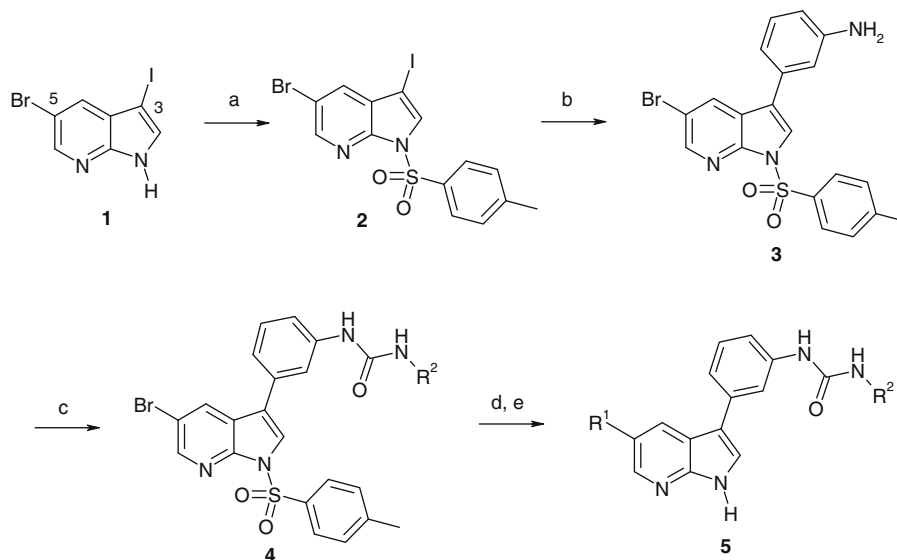
During our efforts to generate leads for the inhibition of protein kinases we identified 3,5-disubstituted-1*H*-pyrrolo[2,3-*b*]pyridines with the general structure **5** as micromolar inhibitors of the IGF-1R tyrosine kinase (Scheme 1). Given that our enzymatic assay was comprised of a GST-fused kinase domain of IGF-1R,⁵ and that the 1*H*-pyrrolo[2,3-*b*]pyridine core⁶ was a known adenine mimic we assumed that the inhibitor's core was binding to the hinge region of the kinase.⁷

* Corresponding author. Present address: NIH Chemical Genomics Center, 9800 Medical Center Dr, Rockville, MD 20850, USA. Tel.: +1 919 4836229; fax: +1 919 4836053.

E-mail addresses: patnaiks@mail.nih.gov, samarjitpatnaik@gmail.com (S. Patnaik).

The synthesis of these inhibitors originated with the known versatile 5-bromo-3-iodo-1*H*-pyrrolo[2,3-*b*]pyridine intermediate **1**,⁶ which was initially protected with *para*-toluenesulfonyl chloride under phase transfer conditions to afford sulfonamide **2**. Chemoselective Suzuki coupling of the iodide **2** with 3-aminophenyl boronic acid was possible at 50 °C with dichlorobis(triphenyl)phosphine palladium and 2*N* aqueous sodium carbonate in a 2:1 mixture of dimethoxyethane and ethanol. This provided aniline **3** which could be functionalized to the urea **4** via addition to various isocyanates. A second Suzuki reaction in a microwave reactor at 120 °C with bromoazaindole **4** was followed by base-mediated hydrolysis of the tosyl group to yield a variety of 1*H*-pyrrolo[2,3-*b*]pyridines. Table 1 lists the inhibitory activities against IGF-1R for a preliminary set of compounds from this series.

Inhibition near micromolar concentrations was observed with unsubstituted phenyl rings at R¹ and R² (**6**) as well as with the 2'-fluoro-4'-trifluoromethyl substituted phenyl ring at R² (**7**). The latter was subsequently crossed with a range of additionally substituted phenyl rings at R¹. While 3',4'-dimethoxy substitution at R¹ (**8**) decreased potency, a moderate improvement was made with 3'-fluoro substitution (**9**). Anilines at the 3'- or 4'-positions (**10**, **11**) improved the enzyme IC₅₀ to more acceptable levels. The homologated congener 4'-benzylamine **12** proved to be 4-fold more potent than the simple aniline **11**. The potency imparted by the 4'-benzylamine substituent was also observed with the



Scheme 1. (a) TsCl, 5 M NaOH, Bu₄NSO₄, CH₂Cl₂, 95%; (b) 3-aminophenylboronic acid, Pd(PPh₃)₂Cl₂, DME/EtOH (2:1), 2M Na₂CO₃, 50 °C, 90%; (c) R²NCO, THF, 60–90%; (d) R¹B(OH)₂, DMF, microwave, Pd(PPh₃)₂Cl₂, 2M Na₂CO₃, 120 °C; (e) 5 M NaOH, MeOH, 50–90% over 2 steps.

3''-chloro phenyl ring at R² as well (compare **18** to **17**). *N*-Methyl piperidine carboxamides at the 3'- and 4'-positions (**13** and **15**) had moderate levels of potency. However, the corresponding unconstrained amides **14** and **16** attained sub-100 nM potencies.

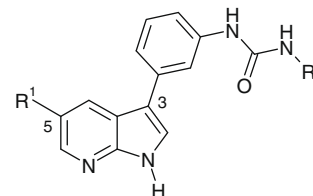
Having discovered groups at R¹ (**12**, **14**, **16**), which imparted nanomolar potencies to the chemical series, we further explored the chemical space at R². In particular, installation of the *ortho*-phenoxy substituent in R² led to the identification of the very potent derivative **19**. This substructure, when crossed with other optimal groups at R¹, further increased the enzymatic activity to single digit nanomolar potencies as exemplified by compounds **20** and **21**. Of particular note was an improvement in kinase selectivity as well. For example, in a preliminary panel of 36 kinases benzyl amine **12** showed >10-fold selectivity against 24 kinases with significant co-activity against IKK1, IKK2, JNK1, JNK3, LYN, and SYK with IC₅₀s measured at 32, 79, 79, 250, 40, and 80 nM respectively. >10-fold selectivity against these six kinases was observed with the related congener **19**. The same trend was exhibited by **20** and **21**. However the *ortho*-phenoxy substructure could not achieve selectivity against the closely related insulin receptor (IR) tyrosine kinase. Having discovered the selectivity imparted by the *ortho*-biphenyl ether for IGF-1R we decided to explore what other groups would be tolerated at R¹. At this time we also developed an assay to measure the cellular activity (phospho IGF-1R Cellular IC₅₀ in Tables 2 and 3) of these inhibitors as well.⁸

With the R² biphenyl ether held constant, we expanded the SAR around R¹. This effort revealed that the above-mentioned enzyme potent derivative **20** was a moderate inhibitor in the cellular assay.⁹ The unsubstituted phenyl ring (**22**) also had mediocre cell potency (Table 2). On the other hand, the 3'-dimethyl carboxamide **23** was a potent IGF-1R inhibitor in the enzyme and cellular assay. The cellular potency for the isosteric 3'-dimethyl sulfonamide **24** was reduced by about 17-fold. A similar trend was observed for the same substituents at the 4'-position (compare **25** to **26**). Carboxylic acid derivatives, whether directly attached to the phenyl ring at R¹ (**27**) or removed from it (**28**), had poor cellular activities. Unsubstituted heterocycles at R¹, for example, furan **29** or imidazole **30**, also affected the cellular potency adversely. All derivatives were essentially equipotent against IR in comparable enzymatic and cellular assays.

A co-crystal of IR (insulin receptor) in complex with **19** offered insight into the binding mode of these inhibitors.¹⁰ Derived from

Table 1

IGF-1R enzyme assay results for **6–21** (values represent an average of ≥ 2 individual measurements)



Compound	R ¹	R ²	IGF-1R enzyme IC ₅₀ (nM)
6			749
7			1262
8			2198
9			605
10			242
11			200

(continued on next page)

Table 1 (continued)

Compound	R ¹	R ²	IGF-1R enzyme IC ₅₀ (nM)
12			50
13			335
14			67
15			286
16			36
17			1015
18			20
19			14
20			4
21			4

this crystal structure, a structural model of IGF-1R in complex with **19** is illustrated in Figure 1. Given that the sequence identity between the kinase domains of IR and IGF-1R is roughly 80%, IR was a reasonable surrogate for IGF-1R, and we concluded that the binding mode of these inhibitors would be nearly identical within the ATP-binding site of both kinases. A frontal view of the IGF-1R ATP-binding site (Fig. 1A) clearly shows that the 1*H*-pyrrolo[2,3-*b*]pyridine core forms two H-bond interactions at the hinge region, one with the backbone carbonyl of Glu1050 and the second

Table 2

IGF-1R enzyme and mechanistic cell assay results for biphenyl ether urea containing compounds **20**, **22**–**30** (values represent an average of ≥ 2 individual measurements)

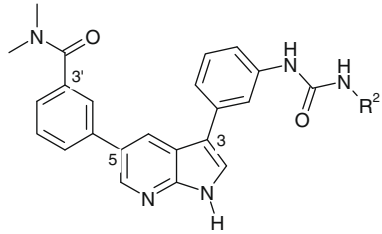
Compound	R ¹	IGF-1R enzyme IC ₅₀ (nM)	Phospho IGF-1R cellular IC ₅₀ (nM)
20		4	415
22		127	693
23		21	68
24		57	1116
25		31	128
26		nd	20,793
27		184	1041
28		210	3623
29		251	1264
30		233	7463

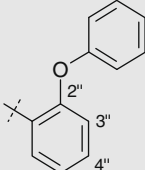
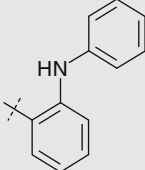
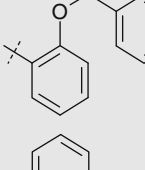
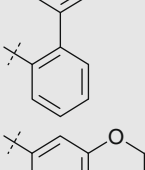
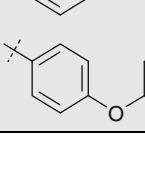
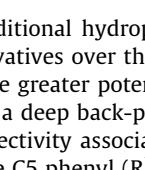
nd, not determined.

with the backbone amino group of Met1052. The C3 phenyl at the 1*H*-pyrrolo[2,3-*b*]pyridine core lies at the inner hydrophobic region where it interacts with Val983, Lys1003, Met1049, Met1112, and Phe1124.¹¹ Near the DFG motif, the urea lies just past the activation loop, where the urea hydrogens interact with one of the carboxylate oxygens of Glu1020 (Fig. 1B). This interaction directs the biphenyl ether deeper into the back-pocket region, where it lies below the α C-helix in contact with Val1023, Met1024, Phe1027, Val1032, Leu1096, Phe1101, His1103, and Ile1121 (Fig. 1B).

Table 3

IGF-1R enzyme and cellular assay results for **23**, **31–35** (values represent an average of ≥ 2 individual measurements)



Compound	R ²	IGF-1R enzyme IC ₅₀ (nM)	Phospho IGF-1R cellular IC ₅₀ (nM)
23		21	68
31		39	407
32		132	517
33		64	385
34		212	961
35		2039	3071

The additional hydrophobic contacts created by the biphenyl ether derivatives over those with a single phenyl may account in part for the greater potency seen with the former over the latter. Also, such a deep back-pocket binding mode may account for the IGF-1R selectivity associated with the biphenyl ether derivatives. Finally, the C5 phenyl (R¹) occupies the outer hydrophobic region with the ionizable primary amine exposed to solvent. At this position, the presence of water solubilizing groups is well tolerated.

With an understanding of the binding mode of the biphenyl ether we decided to elaborate on the SAR around this substructure (Table 3). The C5 3'-dimethyl benzamide substituent was chosen for comparison as it was found to impart high potency in our cellular assay (e.g., **23**, Table 2).¹² The biphenyl aniline isostere **31** lost about 6-fold cellular potency compared to **23**, while maintaining enzyme activity. The homologated 2''-benzyl ether **32** and the directly attached 2''-biphenyl derivative **33** had reduced activity in both enzyme and cellular assays. The movement of the phenoxy

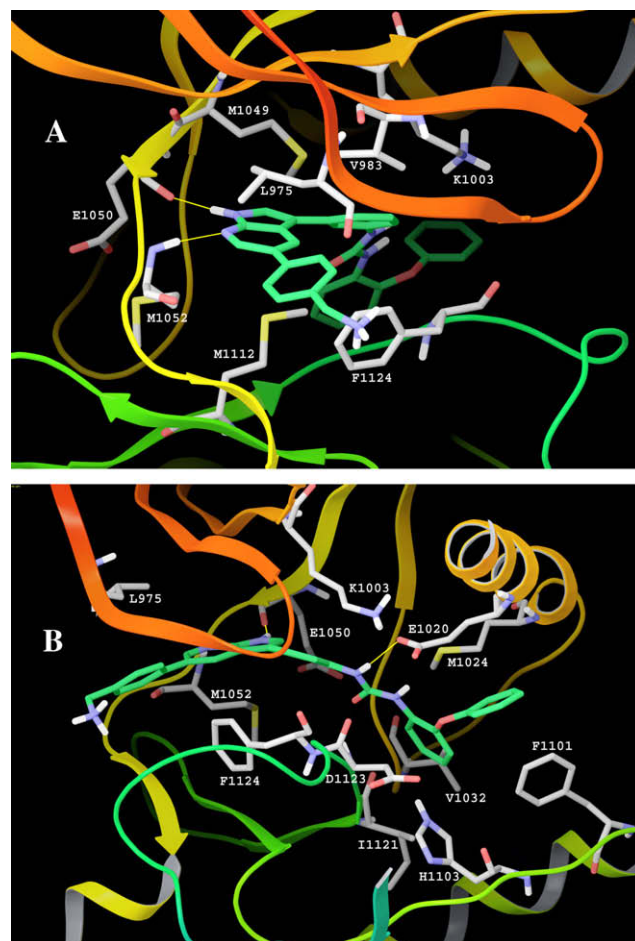


Figure 1. Structural model of IGF-1R (carbons in gray) in complex with **19** (carbons in green). (A) Frontal view of the ATP-binding site. (B) Cross-sectional view of the ATP-binding site and back-pocket region. Intermolecular H-bond interactions are highlighted with yellow lines.

group to meta (**34**) or para (**35**) positions also led to significant losses of potency with respect to **23**. This work implied that the conformation adapted by the 2''-phenoxy phenyl group at R² was optimal in making the appropriate contacts with the hydrophobic residues at the back pocket of the enzyme, as minor deviations away from the structure reduced the effectiveness of this binding mode.

In summary, SAR exploration around the 1H-pyrrolo[2,3-b]pyridine core led to the discovery of potent inhibitors of the IGF-1R tyrosine kinase. These compounds bind to the enzyme such that the 2''-phenoxy ether accesses a unique back pocket in the enzyme. Subtle changes to this pharmacophore led to loss of activity underscoring its unique nature. Additional development within this series of compounds will be discussed in future communications.

References and notes

- Pollack, M. N.; Schernhammer, E. S.; Hankinson, S. E. *Nat. Rev. Cancer* **2004**, *4*, 505.
- Ryan, P. D.; Goss, P. E. *Oncologist* **2008**, *13*, 16 (and references therein).
- Paz, K.; Hadari, Y. R. *Comb. Chem. High Throughput Screen.* **2008**, *11*, 62.
- (a) García-Echeverría, C.; Pearson, M. A.; Marti, A.; Meyer, T.; Mestan, J.; Zimmermann, J.; Gao, J.; Brueggen, J.; Capraro, H. G.; Cozens, R.; Evans, D. B.; Fabbro, D.; Furet, P.; Porta, D. G.; Liebetanz, J.; Martiny-Baron, G.; Ruetz, S.; Hofmann, F. *Cancer Cell* **2004**, *5*, 231; (b) Mulvihill, M. J.; Ji, Q. S.; Coate, H. R.; Cooke, A.; Dong, H.; Feng, L.; Foreman, K.; Rosenfeld-Franklin, M.; Honda, A.; Mak, G.; Mulvihill, K. M.; Nigro, A. I.; O'Connor, M.; Pirrit, C.; Steinig, A. G.; Siu, K.; Stolz, K. M.; Sun, Y.; Tavares, P. A.; Yao, Y.; Gibson, N. W. *Bioorg. Med. Chem.* **2008**, *16*, 1359–1375; (c) Ji, Q. S.; Mulvihill, M. J.; Rosenfeld-Franklin, M.;

- Cooke, A.; Feng, L.; Mak, G.; O'Connor, M.; Yao, Y.; Pirritt, C.; Buck, E.; Eyzaguirre, A.; Arnold, L. D.; Gibson, N. W.; Pachter, J. A. *Mol. Cancer Ther.* **2007**, *6*, 2158–2167; (d) Mulvihill, M. J.; Ji, Q. S.; Werner, D.; Beck, P.; Cesario, C.; Cooke, A.; Cox, M.; Crew, A.; Dong, H.; Feng, L.; Foreman, K. W.; Mak, G.; Nigro, A.; O'Connor, M.; Saroglou, L.; Stolz, K. M.; Sujka, I.; Volk, B.; Weng, Q.; Wilkes, R. *Bioorg. Med. Chem. Lett.* **2007**, *17*, 1091; (e) Saulnier, M. G.; Frennesson, D. B.; Wittman, M. D.; Zimmermann, K.; Velaparthy, U.; Langley, D. R.; Struzynski, C.; Sang, X.; Carboni, J.; Li, A.; Greer, A.; Yang, Z.; Balimane, P.; Gottardis, M.; Attar, R.; Vyas, D. *Bioorg. Med. Chem. Lett.* **2008**, *18*, 1702; (f) Velaparthy, U.; Liu, P.; Balasubramanian, B.; Carboni, J.; Attar, R.; Gottardis, M.; Li, A.; Greer, A.; Zoeckler, M.; Wittman, M. D.; Vyas, D. *Bioorg. Med. Chem. Lett.* **2007**, *17*, 3072; (g) Velaparthy, U.; Wittman, M.; Liu, P.; Stoffan, K.; Zimmermann, K.; Sang, X.; Carboni, J.; Li, A.; Attar, R.; Gottardis, M.; Greer, A.; Chang, C. Y.; Jacobsen, B. L.; Sack, J. S.; Sun, Y.; Langley, D. R.; Balasubramanian, B.; Vyas, D. *Bioorg. Med. Chem. Lett.* **2007**, *17*, 2317; (h) Bell, I. M.; Stirdivant, S. M.; Ahern, J.; Culberson, J. C.; Darke, P. L.; Dinsmore, C. J.; Drakas, R. A.; Gallicchio, S. N.; Graham, S. L.; Heimbrook, D. C.; Hall, D. L.; Hua, J.; Kett, N. R.; Kim, A. S.; Kornienko, M.; Kuo, L. C.; Munshi, S. K.; Quigley, A. G.; Reid, J. C.; Trotter, B. W.; Waxman, L. H.; Williams, T. M.; Zartman, C. B. *Biochemistry* **2005**, *44*, 9430.
5. *IGF-1R enzyme assay.* GST-rTEV-IGF-1R(957–1367) containing amino acid residues 957–1367 was purified from a baculovirus expression system in Sf9 cells using Glutathione Sepharose 4FF column chromatography followed by Sephadex-200 size exclusion column chromatography. Assays were performed in 384-well (Greiner, Catalog No. 784076) microtiter plates. Reaction buffer (50 mM Hepes buffer, pH 7.5; 10 mM MgCl₂; 3 mM DTT; 1 mM CHAPS; 0.1 mg/ml BSA) for peptide phosphorylation (10 μl volume) contained, in final concentrations, 500 nM biotinylated peptide substrate; 10 μM ATP; and purified, activated hIGF-1R (0.5 nM). Activation of GST-rTEV-IGF-1R(957–1367) was achieved by a 4-min incubation of hIGF-1R (2.7 μM final) with 2 mM ATP in 50 mM Hepes, 20 mM MgCl₂, 0.1 mg/ml BSA, at room temperature. Compounds, titrated in DMSO, were evaluated at eleven concentrations ranging from 50 μM to 0.2 nM. Reactions were incubated for 1 h at room temperature and were stopped by a 5-μl addition of EDTA (to 33 mM). A further addition of 5 μl detection reagents (for final 7 nM Streptavidin-APC (Perkin-Elmer #CR130-150), 1 nM Europium-labeled anti-phosphotyrosine monoclonal antibody (Perkin-Elmer #AD0067), added in reaction buffer (without DTT), was required for signal generation. After 30 minutes, signal was read on Perkin-Elmer Viewlux microplate imager or Wallac Victor fluorometer as subtracted from all samples for background).
6. (a) Arnold, W. D.; Bounaud, P.; Gosberg, A.; Li, Z.; McDonald, I.; Steensma, R. W.; Wilson, M. E. US2007043068-A1, 2007.; (b) Arnold, W. D.; Bounaud, P.; Gosberg, A.; Li, Z.; McDonald, I.; Steensma, R. W.; Wilson, M. E. WO2006015123-A1, 2006.; (c) Graczyk, P.; Palmer, V.; Khan, A. WO Patent 2004101565-A2, A3, 2004.
7. For a recent discussion of crystal structures of 1*H*-pyrrolo[2,3-*b*]pyridines bound to protein kinases, see: Tsai, J. et al *Proc. Natl. Acad. Sci. U.S.A.* **2008**, *105*, 3041.
8. *Cell assay.* NIH-3T3 cells overexpressing human IGF-1R were plated in 96-well plates (10,000 cells/well) in culture media containing 10% fetal bovine serum and incubated at 37° C in a 5% CO₂ incubator. Twenty four hours post-plating, cells were treated with different concentrations of test compounds ranging from 30 μM to 1.5 nM. Two hours after compound addition, cells were stimulated with human IGF-1 (30 ng/ml). Cell lysates were analyzed for phosphorylated receptors using dissociation enhanced lanthanide fluorimetric assay (DELFI) with anti-IGF-1R (MAB391, R&D Systems, Minneapolis, MN) capture antibody and europium-labeled anti-pTyr antibody (Eu-N1 PT66, Perkin-Elmer, Waltham, MA) for detection. The fluorescence signal for cells treated with compounds was expressed as percent relative to 100% stimulation (IGF-1 stimulated signal). Concentration of test compound that inhibited 50% of ligand-induced receptor phosphorylation (IC₅₀) was determined by 4 parameter fit of data using XLfit (value of no cell control was subtracted from all samples for background).
9. The cellular potencies of **19** and **21**, reported in Table 1, were not determined.
10. IR protein was expressed and purified as previously described in Hubbard, S. R. et al. *Nature*, **1994**, *372*, 746. Protein at 10 mg/ml was complexed with a 3-fold molar excess of inhibitor for 1 h prior to crystallization. Crystals were grown by hanging drop vapor diffusion at 22° from 0.1 M MOPS, pH 7.0, 1.0 M trisodium citrate. Crystals were flash frozen in PFO prior to data collection. The structure was solved by molecular replacement using PDB:1IRK as a starting model and refined to an R_{factor} of 20% at 2.6 Å using REFMAC. Crystallographic data for the structure in Figure 1 have been deposited at PDB:3ETA.
11. For kinase ATP binding pocket nomenclature, see: Vulpetti, A.; Bosotti, R. *Il Farmaco* **2004**, *59*, 759.
12. Compound **23** inhibited cellular proliferation in a COLO205 cell line with EC50 at 274 nM (average of 4 measurements).